Thermal conductivity of semiconductor superlattices: Experimental study of interface scattering

Jean Yves Duquesne

Thermal conductivity of semiconductor superlattices: experimental study of interface scattering.

J.-Y. Duquesne

Institut des NanoSciences de Paris, UMR 7588

CNRS, Université Pierre et Marie Curie - Paris 6

140, rue de Lourmel

F-75005 Paris - France

Abstract

We present thermal conductivity measurements performed in three short-period $(GaAs)_9(AlAs)_5$ superlattices. The samples were grown at different temperatures, leading to different small scale roughness and broadening of the interfaces. The cross-plane conductivity is measured with a differential 3ω method, at room temperature. The order of magnitude of the overall thermal conductivity variation is consistent with existing theoretical models, although the actual variation is smaller than expected.

PACS numbers: 66.70.-f, 68.65.-k, 68.65.Cd, 44.10.+i

I. INTRODUCTION

The thermal conductivity of semiconductor superlattices is strongly reduced with respect to the bulk values of their constituents [1, 2, 3, 4, 5]. The heat is mainly carried by phonons and two mechanisms can explain the effects of the nanostructuration on thermal transport. According to the first (*intrinsic*) mechanism, the zone-folding involves a modification of the phonon dispersion and allows Umklapp process for low energy phonons [6, 7]. According to the second (*extrinsic*) mechanism, phonons are scattered by imperfections at the interfaces [8, 9]. Of course, both mechanisms can be active but their relative contributions is still under debate, mainly for short period superlattices [10]. The assessement of the interface role relies on discrepancies between theoretical calculations, based on intrinsic mechanisms only, and experimental observations. In order to take into account interfaces defects, some authors [9] combined the phonon dispersion curves arising from zone folding and interface scattering in order to fit experimental results on GaAs/AlAs superlattices [3]. Mini-Umklapp processes were not considered and the phonon mean free path in the layers was supposed to be identical to the corresponding bulk value. These authors derived that 17% of the incident phonons on an interface undergo diffuse scattering, because of interface defects. Recently, other authors solved the Boltzmann's equation in superlattices, beyong the constant relaxation time approximation [10]. They adressed the role of the mini-Umklapp process and computed the contribution of the intrinsic mechanism to the thermal conductivity. Comparing their results with experimental data, they inferred that, in $(GaAs)_3(AlAs)_3$, "the reduction due to extrinsic phonon scattering is roughly three times larger than that due to intrinsic scattering". Molecular dynamics calculations also stressed the importance of interface defects [11, 12]. GaAs/AlAs superlattices were simulated with a simplified structure: the two-atom unit cells of GaAs and AlAs are substituted for single average atoms and the interface defects are obtained by assigning at random the atomic sites in the last monoatomic layer of each superlattice layer to an (average) atom or to the other, with a given probability. A 60% decrease of the thermal conductivity was then predicted in $(GaAs)_7(AlAs)_7$ for a 50% substitution probability [11, 12]. Lastly, the temperature dependence of the thermal conductivity gives clues on interface scattering effects [3].

To our knowledge, no experiment has addressed directly the role of interface imperfections. In this paper, we report on experiments performed in $(GaAs)_9(AlAs)_5$ superlattices

exhibiting different interface width. We have measured their cross-plane thermal conductivity, using the so-called differential 3ω technique, at room temperature [13].

II. EXPERIMENTAL RESULTS

The samples are GaAs/AlAs superlattices grown by molecular beam epitaxy, on GaAs buffers. The nominal widths of GaAs and AlAs layers are 2.5 nm and 1.5 nm, respectively, and the number of GaAs-AlAs periods is 120. Table (I) displays the actual periods determined by X-ray diffraction, versus samples.

Ideal interfaces are infinite atomically flat planes separating pure GaAs and AlAs layers. However, actual interfaces exhibit islandlike structures, characterized by their lateral extent and by their height (in terms of monolayers). Direct interfaces (AlAs grown on GaAs) tend to exhibit large islands (lateral extent from $\sim$ 100 to $\sim$ 1000 nm), whereas inverse interfaces (GaAs grown on AlAs) tend to exhibit smaller islands (lateral extent $\sim$ 0.1 to $\sim$ 10 nm). Compositional fluctuations inside large islands may also occur. The quality of actual interfaces depend on a number of parameters, including growth temperature, interruption time... and are usually characterized either by photoluminescence [14] or by Raman scattering [15, 16]. Photoluminescence is sensitive to large scale fluctuations, whereas Raman scattering is sensitive to small scale fluctuations. Small scale fluctuations lead to an effective concentration profile at the interfaces which can be evaluated by Raman scattering and can be used to characterized the interface width [16, 17].

Our samples were grown under the same conditions, except for the substrate temperature T_s, between 510 and 650 C. In that range, small scale interface fluctuations are very sensitive to the growth temperature [15].

Indeed, the very samples that we have studied were characterized previously by Raman scattering [16]. The intensity and frequency shift of the Raman lines were analyzed in term of interface broadening. Identical broadening was assumed for all interfaces. Table (I) gives the interface width d_0, determined from the analysis of the confined optical modes. The samples are labelled with the same name S1, S2 and S4 as in [16]. Clearly, the interface width increases as the growth temperature increases.

We use the differential 3ω method [13] to measure thermal conductivity of three superlattices, grown on GaAs substrates: S1, S2 and S4. We compare their thermal responses with

the responses of GaAs test samples T1, T2 and T3. Previously, a thin (100 nm) dielectric SiO_2 layer is sputtered on S1, S2, S4, T1, T2 and T3 in order to insure electrical isolation between thermal transducers and samples [18]. The insulating SiO_2 layer is deposited in a same run on the samples and test samples. Moreover, during sputtering, the samples and test samples are mounted on a rotating substrate holder. In this way, the insulating layers thickness is found to be nearly constant on T1, T2 and T3: 104, 102 and 105 nm, as measured by ellipsometry. We extrapolate that insulating layer thickness is constant on S1, S2, S4, T1, T2 and T3, within 1.5%. Thermal transducers are processed by lift-off photolithography and thermal evaporation of gold (200 nm) on a thin chromium adhesion layer (few nm). The typical line width is 30 μm (S1: 35.9 μm, S2: 35.7 μm, S3: 33.1 μm, T1: 28.2 μm, T2: 27.3 μm, T3: 28.0 μm). The line length is 2.5 mm (S1, S2, S4) or 3.0 mm (T1, T2, T3). The ratio of the heater line width to the films thickness is around 50. This ratio is large enough to insure one-dimensional heat flow through the films and measurement of cross-plane conductivities. Indeed, simulations based on [19] confirm that possible anisotropy of the superlattices has negligeable effect on the cross-plane conductivity measurement.

The heater/thermometer line thermal response $T_{2\omega}$, i.e. the in-phase and quadrature components of the temperature oscillation at 2ω, reads [13] :

$$T_{2\omega} = \frac{P}{l\pi\Lambda}\int_0^{+\infty} \frac{\sin^2 y}{y^2\sqrt{y^2+iu^2}}dy + \Delta T \tag{1}$$

where :

$$u = \sqrt{\frac{\omega}{\Omega}} \tag{2}$$

$$\Omega = \frac{2\Lambda}{\rho C w^2} \tag{3}$$

$$\Delta T = \frac{P}{lw}R_c \tag{4}$$

At low frequency, equation (1) can be approximated by [18]:

$$T_{2\omega} \simeq \frac{P}{l\pi\Lambda}\left[-\frac{1}{2}\ln\left(\frac{\omega}{\Omega}\right) + K - i\frac{\pi}{4}\right] + \Delta T \tag{5}$$

$\omega/2\pi$ is current frequency supplied to the line. P is the power supplied to the line at 2ω. Λ, ρ and C are the thermal conductivity, mass density and mass specific heat of the GaAs buffer. ΔT and R_c are the temperature drop and thermal resistance through the insulating

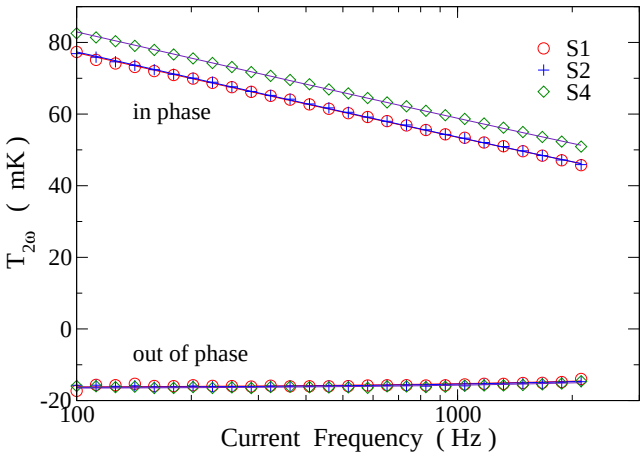

FIG. 1: (Color online) Typical in-phase and out-of-phase temperature oscillations of the heater/thermometer line, versus current frequency. Input power: 3 W.m^{-1}. Symbols: experimental points. Lines: fits using eq.(1).

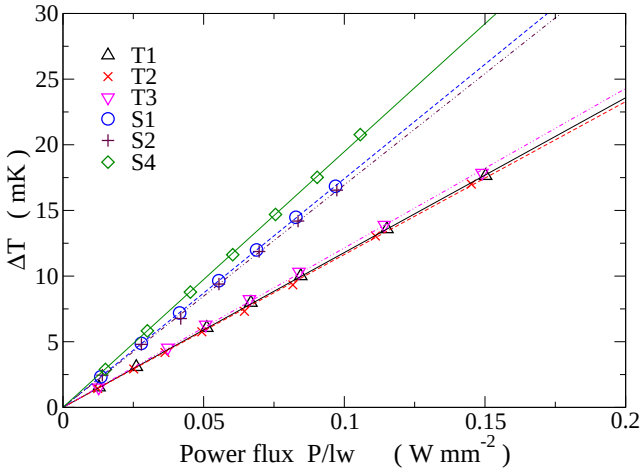

FIG. 2: (Color online) Fitting parameter ΔT (eq.(1)) versus power flux through the heater/thermometer line. Symbols: experimental points. Lines: linear fits.

layer (T1, T2, T3) or through the insulating layer and superlattice (S1, S2, S4). l and w are the length and width of the heater/thermometer line. $K \simeq 0.9066$ is a constant parameter.

The thermal response of the samples and test samples is recorded at $21°C$, versus frequency for P/l ranging from 0.5 to 3.0 $W\ m^{-1}$. We fit experimental data (both in-phase and quadrature components), using equation (1) and two fitting parameters: Λ and ΔT. All the other terms are either measured (l, w, P) or extracted from litterature ($\rho = 5317\ kg\ m^{-3}$,

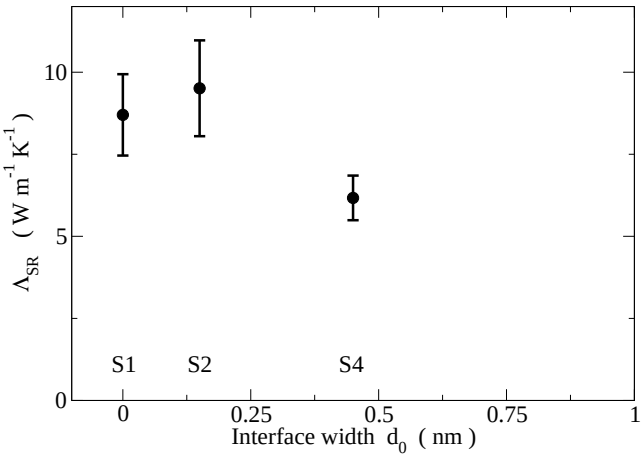

FIG. 3: Thermal conductivity of $(GaAs)_9(AlAs)_5$ superlattices, versus interfaces width.

TABLE I: Sample parameters and experimental results. The superlattices were grown at a substrate temperature of T_s. Their period, interface width [16] and thickness are d, d_0 and e, respectively. R_c is the thermal resistance through SiO_2 layers (T1, T2, T3) or through SiO_2 layers and superlattices (S1, S2, S4). R_{sl} and Λ_{sl} are the superlattice thermal resistance and thermal conductivity.

Sample	T_s	d	d_0	e	$10^7 \times R_c$	$10^7 \times R_{sl}$	Λ_{sl}
	$(°C)$	(nm)	(nm)	(nm)	$(W^{-1}m^2K)$	$(W^{-1}m^2K)$	$(Wm^{-1}K^{-1})$
T1					1.18		
T2					1.16		
T3					1.21		
S1	510	4.01	0	481.2	1.74	0.55	8.7
S2	550	4.01	0.15	481.2	1.69	0.50	9.5
S4	650	3.90	0.45	468.0	1.95	0.76	6.2

$C = 326\ J\ K^{-1}kg^{-1}$ [20]). The uncertainty on ρ and C does not affect our conclusions because the comparison between samples and test samples eliminates the substrate contribution. Figure (1) displays the experimental thermal response $T_{2\omega}$ and fits obtained at $P/l = 3\ W\ m^{-1}$ on S1, S2 and S4. Figure (2) is a plot of the fitting parameter ΔT versus the input power flux $P/(lw)$. For a given sample, the points are aligned and, according to

equation (4), the slope is the thermal resistance R_c. Table (I) summarizes our results.

The thermal resistance R_c through the insulating layer and superlattice (S1, S2, S4) is simply:

$$R_c = R_0 + R_{sl} \tag{6}$$

$$R_{sl} = \frac{e}{\Lambda_{sl}} \tag{7}$$

where R_0 and R_{sl} are the thermal resistances of the insulating SiO_2 layer and of the superlattice. e and Λ_{sl} are the superlattice thickness and thermal conductivity. In order to obtain R_{sl}, we use $R_0 = 1.19\ 10^{-7}\ W^{-1}m^2K$, which is the value we measure on T1, T2, T3 within $\pm 2\%$. Table (I) summarizes our results. Our results lie in the same range as previously reported for GaAs/AlAs superlattices, although direct comparison is hindered by the different periodicities of the samples [3].

The uncertainty on R_c comes mainly from uncertainty on width w of the heater/thermometer line. We estimate $\Delta w = 0.5\mu m$. This induces $\Delta R_c/R_c = 3.2\%$. From those figures, we deduce that layer thermal resistances are nearly equal for S1 and S2 and significantly larger on S4. Actually, we are interested in the variation of Λ_{sl} versus samples. As long as those variations are concerned, R_0 variations from sample to sample must be considered, rather than the actual values and uncertainty on R_0. Those variations come from possible thickness variations and are estimated to be smaller than 2%, in agreement with thickness measurements on T1, T2, T3. Taking into account the uncertainty on the thermal resistance of the layers on S1, S2, S4 and the possible variation of the thermal resistance of the SiO_2 layers, figure (3) displays superlattice thermal conductivity variation, versus interface width. Clearly, S1 and S2 exhibit close thermal conductivities whereas S4 exhibits a significantly smaller thermal conductivity.

Our data analysis neglects the boundary thermal resistances between the various layers (line/insulating film, insulating film/superlattice, superlattice/substrate, insulating film/substrate). However, we may assume the boundary resistances are the same in the various samples. In that case, their contributions are partly cancelled out by the comparison process between samples and test samples. Therefore, the thermal boundary effect may alter the absolute values we derived, but not the overall behavior of the thermal conductivity versus interface width.

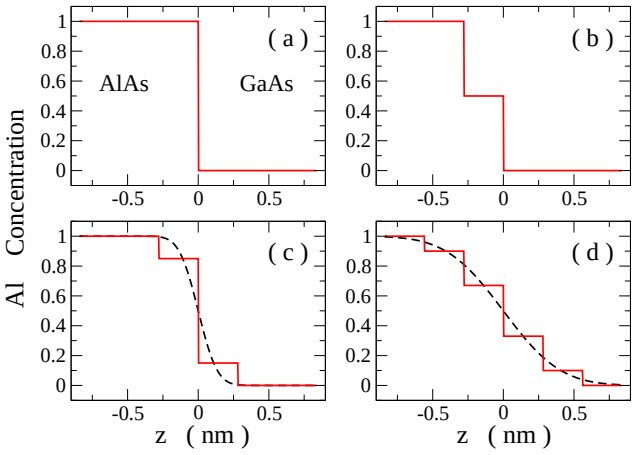

FIG. 4: Aluminium concentration profile versus position along the growth axis z. (a) Perfect interface. (b) according to [11, 12]. (c) $d_0 = 0.15\ nm$. (d) $d_0 = 0.45\ nm$. (c) and (d): dashed line: 'erf' profile according to [16]. Full line: average concentration in the monolayers.

III. DISCUSSION

Clearly, our experiments show that S1 and S2 exhibit close thermal conductivities whereas S4 exhibits a significantly smaller thermal conductivity (30% decrease).

In $(GaAs)_9(AlAs)_5$, the superlattice period d is much smaller than the thermal phonon mean free path l in the bulk constituents ($d = 4\ nm$ and $l \sim 70\ nm$ [9]). In this so called "short period superlattice" regime, we expect the interface defects to modify significantly the phonons mean free path and, as a consequence, the thermal conductivity. This is confirmed by molecular dynamics calculations. Direct comparison of our experimental results with quantitative models is difficult because existing calculations use simplified models for both structure and interfaces [9, 11, 12]. However, we may compare the transition layer at the interfaces involved in both models and experiments. Figure (4) is a sketch of the interface transition layers. In our experiments, S1, S2 and S4 are characterized by an interface width d_0 [16]. From d_0, we may infer the foreign atoms concentration in the transition layer. In S2, $d_0/x_c = 0.5$ ($x_c = 0.28\ nm$ is the monolayer thickness) and the transition layer is two monolayers in thickness: the first and last monolayer at the interfaces. In both monolayers, the foreign atoms concentration is 15%. In S4, $d_0/x_c = 1.6$ and the transition layer is four monolayers in thickness: the first and last two monolayers at the interfaces. In the monolayers the closest to the interfaces, the foreign atoms concentration is 33%. In the

next monolayers, the foreign atoms concentration is 10%. In existing molecular dynamics calculations, the transition layer is one monolayer in thickness. It is located at the last atomic layer in each superlattice layer and the foreign atoms concentration is 50%. A 60% reduction of the thermal conductivity is then inferred in $(GaAs)_7(AlAs)_7$ [11, 12]. On the basis of the above comparison, we conclude that our samples lie in a range where the interface damage should indeed have an impact on the thermal conductivity of our samples.

Large changes of the total phonon mean free path and of the thermal conductivity have been predicted when diffuse scattering is introduced at the interfaces [9]. The largest sensitivity is achieved for small amounts of diffuse scattering. Therefore, the conductivity variation between S1 and S2 is surprisingly small. The conductivity variation which is observed between S1 and S4 is consistent with the order of magnitude predicted from molecular dynamics. However, the 30% variation which is measured appears to be quite small with respect the 60% variation predicted for a less severe interface damage.

IV. CONCLUSION

We have measured the cross-plane thermal conductivity of three short-period $(GaAs)_9(AlAs)_5$ superlattices, at room temperature. Due to different temperature growth, the samples exhibit different small scale roughness at the interfaces. The small scale roughness is characterized by an effective interface width d_0, on the basis of previous Raman scattering experiments. Within error bars, no variation of thermal conductivity is observed between $d_0 = 0$ and $d_0 = 0.15\ nm$, and a 30% decrease is observed between $d_0 = 0$ and $d_0 = 0.45\ nm$. On the basis of existing calculations, the sensitivity of the thermal conductivity to the small scale interface roughness seems to be not as strong as expected. Additional experiments, as well as more realistic calculations must be performed to clarify this point.

Acknowledgement

I am grateful to B. Jusserand for providing samples and for fruitful discussions.

[1] T. Yao, Appl. Phys. Lett. **51**, 1798 (1987).

[2] S.-M. Lee, D. G. Cahill, and R. Venkatasubramanian, Appl. Phys. Lett. **70**, 2957 (1997).

[3] W. S. Capinski, H. J. Maris, T. Ruf, M. Cardona, K. Ploog, and D. S. Katzer, Phys. Rev. B **59**, 8105 (1999).

[4] R. Venkatasubramanian, Phys. Rev. B **61**, 3091 (2000).

[5] S. T. Huxtable, A. R. Abramson, C. L. Tien, A. Majumdar, C. LaBounty, X. Fan, G. Zeng, J. E. Bowers, A. Shakouri, and E. T. Croke, Appl. Phys. Lett. **80**, 1737 (2002).

[6] S. Y. Ren and J. D. Dow, Phys. Rev. B **25**, 3750 (1982).

[7] M. V. Simkin and G. D. Mahan, Phys. Rev. Lett. **84**, 927 (2000).

[8] G. Chen, Phys. Rev. B **57**, 14958 (1998).

[9] B. Yang and G. Chen, Phys. Rev. B **67**, 195311 (2003).

[10] A. Ward and D. A. Broido, Phys. Rev. B **77**, 245328 (2008).

[11] B. C. Daly, H. J. Maris, K. Imamura, and S. Tamura, Phys. Rev. B **66**, 024301 (2002).

[12] K. Imamura, Y. Tanaka, N. Nishiguchi, S. Tamura, and H. J. Maris, J. Phys.: Condens. Matter **15**, 8679 (2003).

[13] D. G. Cahill, M. Katiyar, and J. R. Abelson, Phys. Rev. B **50**, 6077 (1994).

[14] M. A. Herman, D. Bimberg, and J. Christen, J. Appl. Phys. **70**, R1 (1991).

[15] D. Gammon, B. V. Shanabrook, and D. S. Katzer, Phys. Rev. Lett. **67**, 1547 (1991).

[16] B. Jusserand, F. Alexandre, D. Paquet, and G. Le Roux, Appl. Phys. Lett. **47**, 301 (1985).

[17] B. Jusserand, F. Mollot, J.-M. Moison, and G. L. Roux, Appl. Phys. Lett. **57**, 560 (1990).

[18] S.-M. Lee and D. G. Cahill, J. Appl. Phys. **81**, 2590 (1997).

[19] T. Borca-Tasciuc, A. R. Kumar, and G. Chen, Rev. Sci. Instrum. **72**, 2139 (2001).

[20] J. S. Blakemore, J. Appl. Phys. **53**, R123 (1982).